

Facile Synthesis of Silica Coated Magnetic Nanoparticles via Green Microwave-Solventless Technique for Purification of Water from Toxic Heavy Metals

Salwa A Ahmed*, Karima M Zaki and Ezzat M Soliman

Chemistry Department, Faculty of Science, Minia University, Minia, Egypt

Abstract

Silica coated magnetic nanoparticles (SCMNPs) were synthesized via microwave technique and used for removal of Cd(II), Zn(II), and Co(II) ions from water samples. These synthesized nanoparticles were characterized using Fourier Transforming Infrared (FT-IR), X-Ray Diffraction (XRD), Scanning electron microscopy (SEM), and Transmission electron microscopy (TEM). Effects of variables such as pH, contact time, weight of nano-adsorbent, and concentration of the target metal ion on metal uptake capacity have been studied to obtain the optimum conditions. The results recorded metal uptake values to be 2.314, 1.950, 1.780 mmol/g for Cd(II), Zn(II), and Co(II), respectively. The equilibrium data were fitted well with Freundlich model. Kinetic study showed well agreement with the pseudo-second-order one. SCMNPs has been applied to remove Cd(II), Zn(II), and Co(II) from real water samples with quantitative recovery. Finally, regeneration of SCMNPs reached 10 times with the same efficiency; and also found to be very stable under acidic conditions.

Keywords

Heavy metals, Isotherm, Magnetite, Microwave, Nano-adsorbent, Removal, Silica

Introduction

Nano-adsorbents are nanoscale particles or nanocomposites from organic/inorganic materials that have high affinity to absorb substances due to small size and high surface area [1]. They are distinguished by their large surface area and having unique properties and potential applications, especially in water treatment [2]. However, the removal of nano-adsorbent from water solutions is difficult for the small size of these particles. So, magnetic nanoparticles overcome this defect by removing these nanoparticles (NPs) and hazardous elements

adsorbed using an external magnet [3]. The magnetic separation method is effective and has little cost in many areas such as environmental applications, large-scale water purification, sewage treatment, nuclear industry, food production, pharmaceutical and biochemical activities [4]. Iron oxide is one of the most important magnetic nano-sized materials. It has a major role in many areas of chemistry and materials science, in addition to the appropriate magnetic properties, cheapness, and low toxicity [5]. Unfortunately, uncoated magnetic nano-sized iron-oxides have many defects. They are likely to agglomerate in aqueous solutions accordingly,

*Corresponding author: Prof. Dr. Salwa A Ahmed, Chemistry Department, Faculty of Science, Minia University, Minia, Egypt

Accepted: June 04, 2020; Published: June 06, 2020

Copyright: © 2020 Ahmed SA, et al. This is an open-access article distributed under the terms of the Creative Commons Attribution License, which permits unrestricted use, distribution, and reproduction in any medium, provided the original author and source are credited.

Ahmed et al. *Int J Nanoparticles Nanotech* 2020, 6:036

ISSN 2631-5084



9 772631 508002

magnetic properties change and biodegrade in biological systems, it was also found that the bare magnetic nano-adsorbent were exposed to oxidation and loss of its magnetic properties at pH lower than 4 [3]. So, coating of magnetic NPs with silica is a commonly used procedure to obtain magnetic sorbents; this is due to silica stability and versatility of its surface modification [6]. Silica coated magnetic nanoparticles with a magnetic core and a silica shell has the advantages of both materials with no apparent effect on magnetic properties that characterize the nano-magnetite [3]. Using of this magnetic nano-adsorbent for removal of pollutants from water continues to progress nowadays. Heavy metals are considered to be the most hazardous pollutants in the environment [7]. Recently, heavy metals have spread in the environment as a result of various human activities such as metal plating facilities [8], metal finishing, welding and alloy manufacturing [9], mining, fossil fuel combustion and poor sewerage systems, fertilizer industries tanneries, batteries, paper industries and pesticides, etc. Waste water containing heavy metals is often discharged directly or indirectly into the environment, especially in developing countries [8,9]. In living organisms, heavy metals - differ from some organic pollutants - become toxic and non-metabolized when their concentration exceeds the tolerance limit, so the metal bioaccumulates in the soft tissues. Heavy metals can enter the human body through water, food, air or through skin absorption [10]. Furthermore, providing safe drinking water is the key to protecting human health. The presence of these heavy metals, even at low concentrations, is a threat and a real danger to the sources of clean water [11]. About 25% of recent human diseases occur due to long-term exposure to environmental pollutants; this is what has been appreciated by the World Health Organization (WHO) [12]. For example, zinc is one of the most hazardous pollutants that affect human health, among the symptoms of zinc poisoning there are nausea, stomachache, dehydration, electrolyte imbalance, dizziness and in coordination in muscles [13]. Cobalt also has significant health effects, cobalt poisoning causes heart damage causing heart failure, asthma, damage of the thyroid and liver, may also cause genetic mutations, and exposure to ionized radiation increases risk of developing cancer in living cells [14]. Furthermore, cadmium poisoning causes serious diseases,

such as pulmonary fibrosis, renal tubular abnormalities, chronic renal injury and an increased risk of cancer [15]. Therefore there is an urgent need to remove and identify those heavy metals from the environment [9].

There are many techniques and processes that have been used to remove heavy metals from water such as precipitation, ion exchange, evaporation, electrochemical treatments, membrane filtration, flocculation, reverse osmosis, evaporation, flotation, and oxidation. Most of these techniques have their disadvantages [2,11]. For example, precipitation is ineffective when metal ion concentration is low, is not economical and can produce large amount of sludge to be treated with great difficulties. Ion exchangers need to be renewed when they are exhausted and the regeneration can cause serious secondary pollution, and it is expensive. Electrochemical treatments, flocculation and membrane filtration is a high cost techniques, process complexity, membrane fouling and low permeate flux. On the contrary, adsorption is an ideal technique to remove toxic pollutants from water for its simplicity, high efficiency, ease of operation, regeneration characteristics [3], and can remove heavy metals found in water at low concentrations [16]. Fortunately, the evolution of nanotechnology has highlighted this issue [2]. Many researchers used silica coated magnetite and attended it by many methods. From these methods One-Pot Solvothermal process which need very high temperatures and takes about 12 hours and need solvents [17]. Also, among SCMNPS preparation methods there are electrochemical and sol gel methods which are complicated and expensive techniques [18].

In our current study, the silica coated magnetic nanoparticles (SCMNPs) were synthesized using simple and fast household microwave synthesis technique with only a few drops of water (without need to use harmful solvent). The structural, physical and chemical properties of SCMNPs were analyzed; its efficiency has been tested in removing of Cd(II), Zn(II), and Co(II) ions from aqueous solutions under different variables. In addition, the possibility of reusing SCMNPs has been carried out more than 10 consecutive times with the same efficiency and its high stability has been recorded at acidic medium. Finally, water samples from different sources were purified from heavy metals as an application of using this nano-adsorbent in the environment.

Experimental

Materials

Ferric chloride ($\text{FeCl}_3 \cdot 6\text{H}_2\text{O}$) with 98% purity and ferrous sulphate ($\text{FeSO}_4 \cdot 7\text{H}_2\text{O}$) with 98% purity were purchased from Oxford, India. The silica gel used was of TLC grade (70-230 mesh size and 60 Å pore diameter), purchased from Woelm pharm, Eschwege, Germany. 0.1M of stock acidified solutions of $\text{CdCl}_2 \cdot 2\text{H}_2\text{O}$, $\text{ZnCl}_2 \cdot 2\text{H}_2\text{O}$, and $\text{CoCl}_2 \cdot 2\text{H}_2\text{O}$ were prepared by dissolving 13.629, 20.132, and 15.5 g, respectively in 1.0 liter measuring flask using double distilled water (DDW) (a small amount of HCl (1M) was added for each metal ion solution to avoid the hydrolysis). These metal salts were of analytical grade purchased from Aldrich (USA), BDH (England) or Prolabo (Egypt). Methylthymol blue and xylenol orange used as indicators for complexometric EDTA titration. HCl and NaOH used for justifying the pH values were purchased from Aldrich chemical Co., USA. Water samples including: Nile River water (NRW), ground water (GW) were collected from Minia governorate, Egypt, drinking tap water (DTW) from Minia university, and sea water (SW) was collected from Alexandria governorate, Egypt.

Instruments

The FT-IR-spectra of (SCMNPs) was recorded by Shimadzu Affinity A₁ FT-IR spectrophotometer (Japan) using KBr pellets and expressed as $\text{U}_{\text{max}} \text{cm}^{-1}$. A Fisher Scientific Accumet pH-meter (Model 825) (Germany) calibrated against two standard buffer solutions at pH 4.0 and 9.2 were used for all pH measurements. Atomic absorption measurements for measuring concentrations of metal ions were performed with Aquanova-Genway spectrometry (UK). Wrist Action mechanical shaker Model 75 (manufactured by Burrell Corp., Pittsburgh, PA, USA) was used for the shaking process. Microwave oven (KOR-131G, Korea) emitting 2450 MHz, voltage: 230 V, frequency: 50 Hz, input power: 1650 W, energy output: 1100 W was used for the synthesis of the novel SCMNPs. X-ray Diffraction (XRD) analysis for proving the crystal phase of the magnetic composite was carried out by JEOL X-ray diffractometer system, model JDX-9C specification (Japan). The size, morphology and structure of nano-adsorbent were characterized by JEOL GEM-1010 transmission electron microscope (TEM) at 70 kV (Japan) at the Regional Center of Mycology and Biotechnology,

Al-Azhar University, Cairo, Egypt. The micrographs of prepared particles were obtained using scanning electron microscopy (SEM) (model: JSM-5500 LV; JEOL Ltd -Japan) by using high vacuum mode at the Regional Center of Mycology and biotechnology, Al-Azhar university, Cairo, Egypt.

Synthesis of the magnetic nano-adsorbent

Preparation of magnetic nanoparticles: Magnetic nanoparticles were prepared by the co-precipitation method, by slow addition of 5M NaOH solution into a mixed solution of 0.25M $\text{FeSO}_4 \cdot 7\text{H}_2\text{O}$ and 0.5M $\text{FeCl}_3 \cdot 6\text{H}_2\text{O}$ till obtaining pH 11, at room temperature. The magnetite particles thus formed were left to settle, then magnetically separated from the supernatant where they thoroughly washed with doubly distilled water till reaching neutral medium [19,20]. Finally, they collected and dried in an oven at 60 °C. The Fe_3O_4 -MNPs thus produced using this method was dense, dark brown and magnetic with a particle size in range 13.3-29.2 nm.

Silica coated magnetic nanoparticles: An advanced method has been developed for this purpose, where a solid - solid interaction is performed under solvent-less microwave condition. Thus, Fe_3O_4 - MNPs were mixed with silica in weight/weight ratios (w/w = 1:1). These mixtures were individually grinded using mortar of agate, wetted with drops of distilled water and then microwaved at actual power 200 w for 20 min. The produced nano-adsorbents were dry and homogeneous with color of dark brown of silica coated magnetic nanoparticles (SCMNPs) see graphical Scheme 1.

Parameters affecting metal uptake capacity

The metal uptake capacity of SCMNPs towards Zn(II), Cd(II), and Co(II) ions were determined in triplicate under static conditions by the batch equilibrium technique. In which 25 mg of SCMNPs were added to 1 ml of 0.1M of metal ion solution at pH range of 1.0 to 6.0, except for Zn(II), where the pH used at 1.0 to 8.0; the total volume was completed to 50 ml by DDW in a 100 ml measuring flask, for pH adjustment, solutions of 0.1M HCl and 0.1M NaOH were used. The mixture was mechanically shaken for 10 min at room temperature to reach equilibrium. Then, the nano-adsorbent was separated by an external magnet and washed with DDW; the un-retained metal ion in the filtrate was determined by complexometric EDTA titration. The equation of

metal uptake capacity could be obtained as follow:

$$Q_e = (C_o - C_e) V/m \quad (1)$$

Where, C_o , and C_e are initial concentration of metal ion (mmol/mL) and the equilibrium concentration of unadsorbed metal ions in the decanted solution (mmol/mL), respectively, V is the volume of solution (mL) and m is the nanocomposite mass in grams (g). Finally, Q_e is metal uptake capacity (mmol/g) [21].

Moreover the effect of contact time on metal uptake was determined under the same conditions for different equilibrium periods (2, 5, 10, 20, and 30 min) at the pH of the highest metal ion uptake (optimum pH value). Effect of weight was determined for different weights (10, 25, 35, and 50 mg) of nano-adsorbent, and effect of concentration was determined for different concentrations of metal ion ranging from 2×10^{-4} to 2×10^{-3} M.

Stability studies (Effect of medium)

The study of prolonged medium effects on the adequacy of SCMNPs is important from practical application point of view. It was investigated under static conditions, different concentrations (0.1, 0.3, and 0.5M) of HCl prepared, mixed with definite weights of nano-adsorbent and shaking the mixture for 30 min. To increase the emphasis on the nano-adsorbent stability, another definite weight was impregnate with 0.1M HCl overnight. The treated SCMNPs was filtered, washed with DDW and dried at 60 °C for 6 h. Then, evaluate the metal ion sorption capacity at the optimum pH values using the batch technique under the same conditions as previously described. Finally, the results have been compared with the standard untreated one to follow the hydrolysis of the nano-adsorbent.

Regeneration of the nano-adsorbent

To investigate the extent to which SCMNPs could be used more than once to extract the metal after first use, ethylenediaminetetraacetic acid (EDTA) was used as a strong complexing agent to recover the metal from the surface of the SCMNPs by a batch recycling process. Thus, 100 mg of SCMNPs after adsorption of metal ion at optimum pH values was mixed with excess of 0.1M EDTA solution. Then, they are shaken for an hour, filtered, washed with DDW many times and dried at 60 °C for 6 h to evaluate the ability of SCMNPs to be reused.

Result and Discussion

Characterization of silica coated magnetic nano-adsorbent

FT-IR analysis: The FT-IR spectra of silica, Fe_3O_4 , and Fe_3O_4/SiO_2 , are shown in Figure 1 for determination of variation frequency changes in the range of 4000-400 cm^{-1} . (Figure 1a) illustrates the spectrum of silica gel in which appear a strong and sharp peak of Si-O bond at 1100 cm^{-1} , the peaks at 480 cm^{-1} are ascribed to the Si-O-Si bending vibration, also a strong peak of the silanol groups appear at 3444.82 cm^{-1} . The characteristic wavenumbers of 625 and 575 cm^{-1} corresponds to the Fe-O bonds, which is reported to belong to bulk magnetite, (Figure 1b). Finally, the FT-IR spectrum of SCMNPs as shown in (Figure 1c) was measured to demonstrate the coverage of the surface of magnetite by silica gel. The deposition of silica network on the magnetite surface by Fe-O-Si bonds was confirmed by obtaining relevant FT-IR spectrum. The corresponding absorption band cannot be seen in the FT-IR spectrum because it appears at around 580 cm^{-1} and inevitably overlaps with the Fe-O vibration of magnetite, it also shows appearing of peaks of bulk magnetite (Fe_3O_4) stretching vibration with a slight deviation to right. On the other hand, the strong and sharp peaks appeared and shifted at approximate 1000.43 and 3412.86 cm^{-1} belongs to Si-O bond and silanol groups of silica gel, respectively. The final product which obtained as dense, dark brown and has magnetic properties implying complete coverage of the surface of magnetite core by a shell of silica gel [22,23].

X-ray diffraction, Scanning electron microscope (SEM), and transmission electron microscope (TEM): XRD patterns of silica, magnetite, and SCMNPs were obtained in Figure 2. The XRD peaks of magnetite show characteristic diffraction line at 2θ range of 25-65° as shown in Figure 2a. Peaks of silica appear about 2θ range of 8-27°, (Figure 2b). Finally by studying the XRD of SCMNPs, as shown in Figure 2c, new diffraction lines were observed at 2θ range of 15-64°, shows the peaks for SCMNPs with differences in the intensity and shape of the peaks. These changing in diffraction lines are favor to prove immobilization of the magnetite core with a silica shell.

The morphological shape of the silica magnetite surface was analyzed by using scanning electron microscope (SEM) as illustrated in Figure 3. The image contains large particles with a rough surface

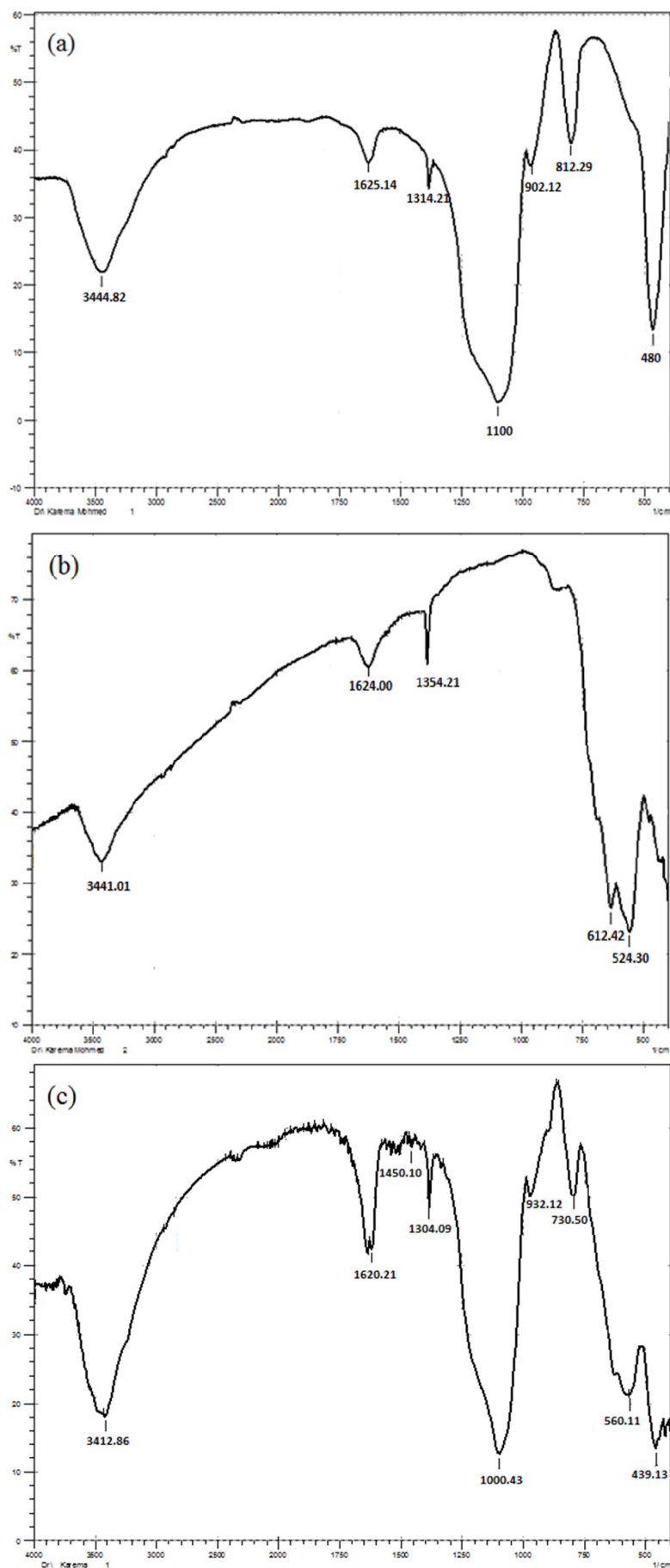


Figure 1: FT-IR spectra of a) Silica; b) Fe_3O_4 -MNPs, and c) SCMNPS.

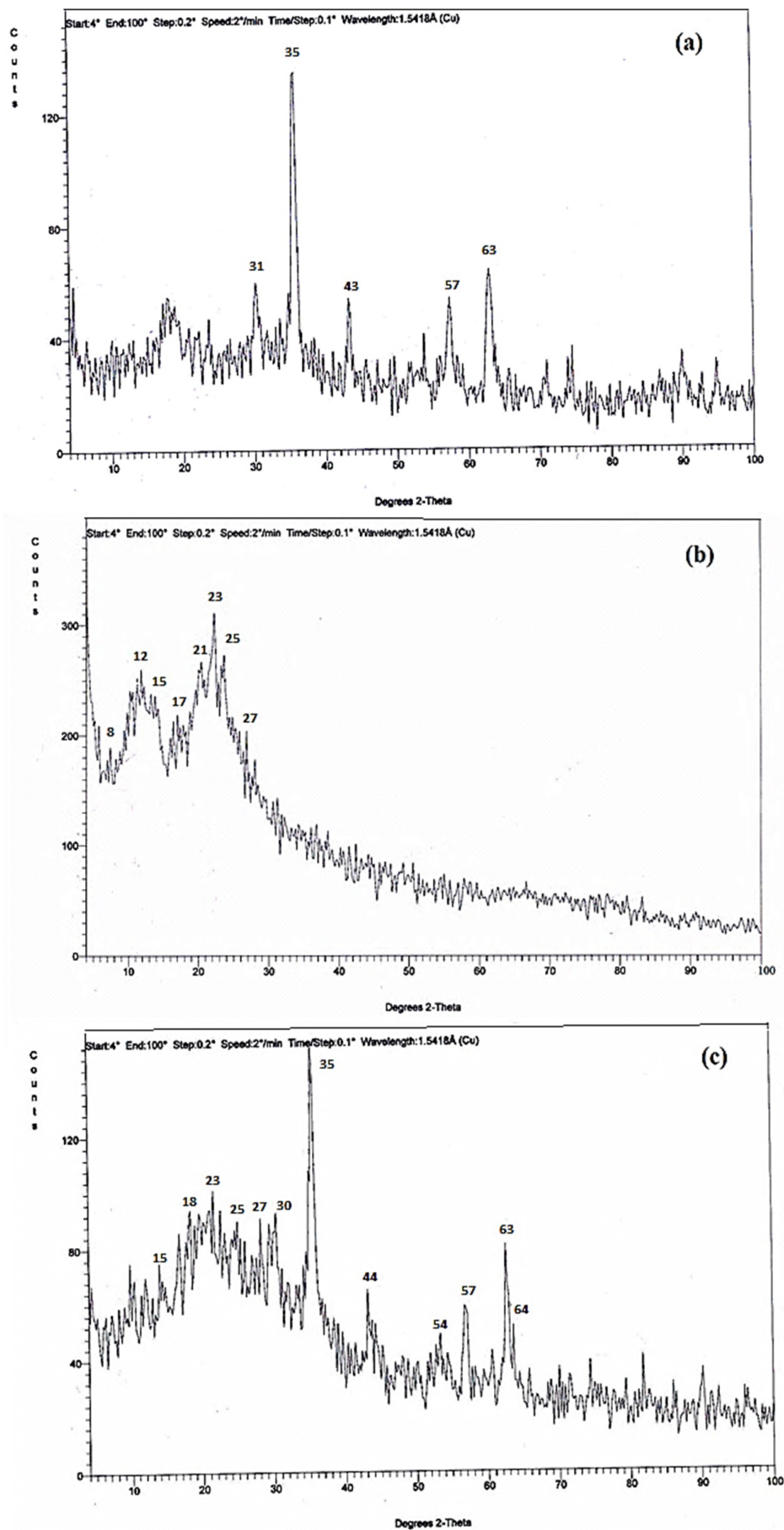


Figure 2: X-ray diffraction for a) Fe_3O_4 .MNPs; b) Silica, and c) SCMNPs.

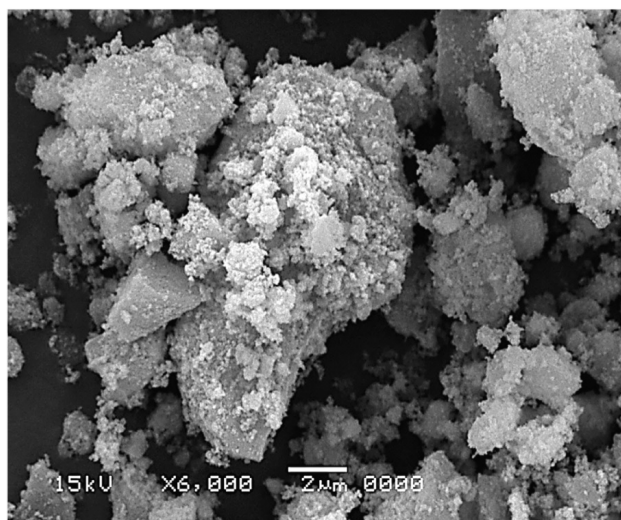


Figure 3: SEM images of SCMNPs.

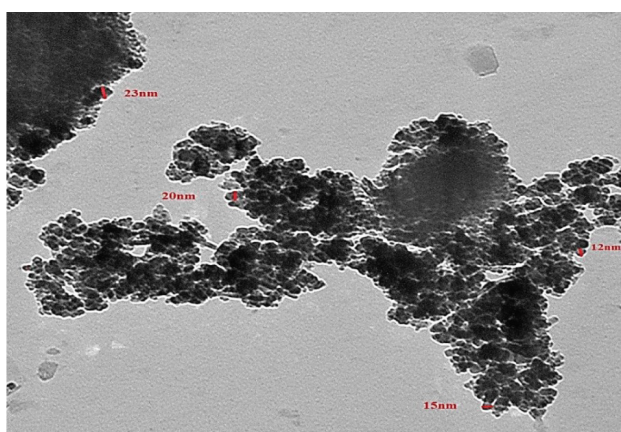


Figure 4: TEM images of SCMNPs.

and good homogeneity in the distribution with respect to particle size and shape. These large particles represent an important factor in facilitating the process of mass transfer rate of metal ions to be adsorbed on the surface of SCMNPs, and so get better adsorption capacity.

The size and structure of SCMNPs were characterized using TEM micrographs, **Figure 4**. Practical experiments have demonstrated the presence of spherical particles, and as observed that there are black magnetite cores and a thin shell of silica coating it. Molecule diameter is at the range of 11.7–24.81 nm with the mean size of 16.93 nm.

Adsorption studies

Effect of pH: The study of the effect of pH of the solution has been found to have a significant impact on metal adsorption on the surface of SCMNPs. The

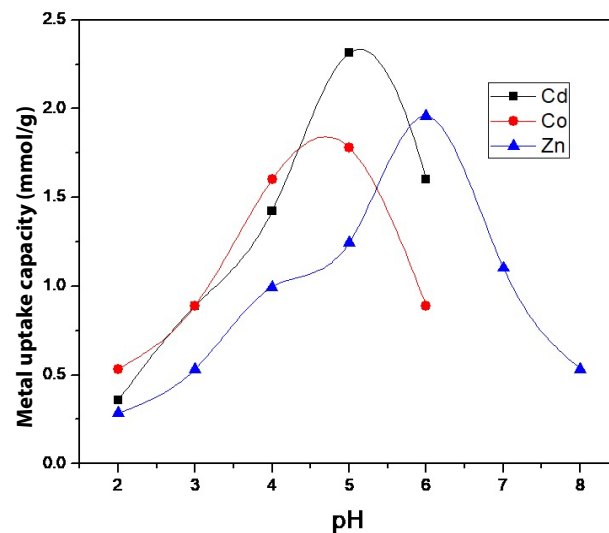


Figure 5: Effect of pH on metal uptake capacity of Cd(II), Co(II), and Zn(II) using SCMNPs.

pH effect was studied over the pH range from 1.0 to 8.0 by the batch equilibrium technique under static conditions. As shown in **Figure 5**, there is low efficiency toward the extraction of heavy metal at low pH values; there is a large amount of hydrogen ions so a competition occurs between metal ions and hydrogen ions on the binding sites, resulting in decrease of metal ions binding. By increasing the value of pH the competition become weaker so metal uptake capacity increase until it reach its optimum value at 5.0 for Cd(II) and Co(II), and 6.0 for Zn(II). The values of metal uptake capacity at the optimum pH for Cd(II), Zn(II), and Co(II) were 2.314, 1.952, and 1.780 mmol/g, respectively. By increasing the pH value more than 6.0, metal uptake capacity go back again to decline due to the presence of excess amount of hydroxide ion. The predominant metal species at pH between 2.0 and 7.0 are positively charged $[M^{n+}]$ and $[M(OH)^{(n-1)+}]$, therefore, uptake of metals may proceed through Mn^+ exchange process with acidic sites H^+ , complexing with functional groups and/or chelation [24]. Finally, the affinity of SCMNPs for binding to the studied heavy metal ions can be arranged based on their uptake values according to the following order: Cd(II) > Zn(II) > Co(II).

Effect of contact time: The effect of contact time was studied over a variety of times (2, 5, 10, 20, and 30 min) at the optimum pH value for each studied metal. Determination of the equilibrium contact time is an important parameter not only for the adsorption process, but also for the oper-

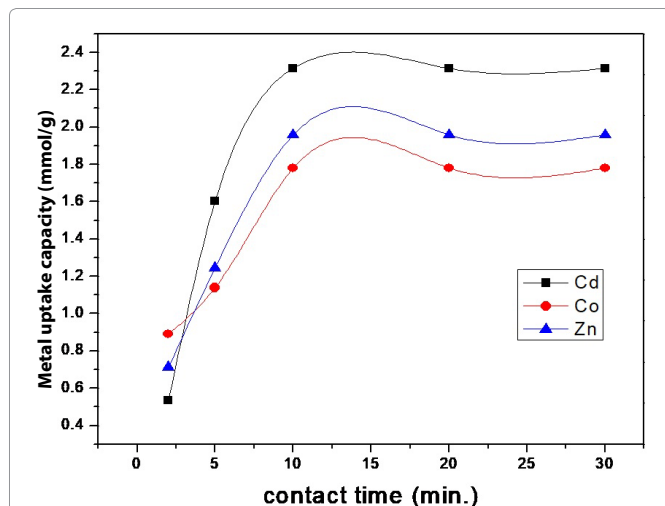


Figure 6: Effect of contact time on metal uptake capacity of Cd(II), Co(II), and Zn(II) using SCMNPs.

ational cost, **Figure 6**. It was clearly indicated that the rate of adsorption was very fast and the equilibrium was reached within 10 min of contact time and then reached to a saturation level. The adsorption process was fast at the beginning stages because of the availability of vacant binding sites on SCMNPs composite as the time passed; these active sites became more reacted and covered with metal ions, which restricted further binding of ions. The short equilibrium time (10 min) provides an economic advantage for extensive application because it means less energy consumption and reduction of production cost [25]. Therefore, metal uptake capacities at 10 min (optimum time) for Cd(II), Zn(II), and Co(II) were 2.314, 1.952, and 1.870 mmol/g, respectively.

A kinetic model was created to study the mechanism of removal of metals and its potential rate-controlling steps to analyze the experimental data. The sorption kinetic data was analyzed in terms of pseudo-first-order and pseudo-second-order sorption equations. The equation of the pseudo-first-order is shown below:

$$\frac{dq_t}{dt} = k_1 (q_e - q_t) \quad (2)$$

Where, q_t (mmol/g) refer to the amount of sorption at time t (min), q_e (mmol/g) is the amount of sorption at equilibrium, and k_1 (min^{-1}) is the rate constant of the pseudo-first-order sorption. After doing integration and at the conditions of $q_t = 0$ at $t = 0$ and $q_t = q_t$ at $t = t$, Eq. (2) becomes:

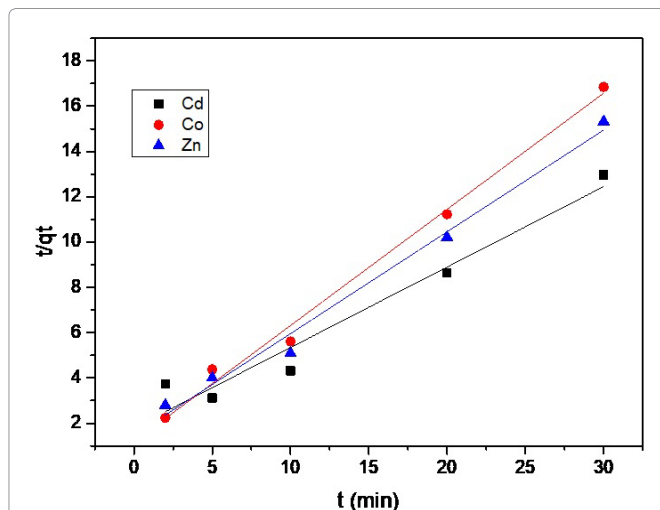


Figure 7: Pseudo-second-order kinetic plot for the adsorption capacity of Cd(II), Zn(II), and Co(II) using SCMNPs.

$$\log(q_e - q_t) = \log q_e - \left(\frac{k_1}{2.303} \right) t \quad (3)$$

But this model cannot be applied because there is no correlation with the experimental data, so it is not appropriate to describe the entire process. So, the adsorption kinetic data analyzed also in terms of pseudo-second-order sorption equation which is shown below:

$$\frac{dq_e}{dt} = k_2 (q_e - q_t)^2 \quad (4)$$

Here, k_2 ($\text{g}/\text{mmol}/\text{min}$) is the rate constant. By integration of this equation and application at conditions of $q_t = 0$ at $t = 0$ and $q_t = q_t$ at $t = t$, Eq. (4) becomes:

$$\frac{1}{q_e} - \frac{1}{q_t} = \frac{1}{q_e} + k_2 t \quad (5)$$

By rearrangement of Eq. (5) to give the linear form as follows:

$$\frac{t}{q_t} = \frac{1}{v_o} + \left(\frac{1}{q_e} \right) t \quad (6)$$

Where, $v_o = kq_e^2$ ($\text{mmol g}^{-1} \text{min}^{-1}$) is the initial sorption rate, k ($\text{g mmol}^{-1} \text{min}^{-1}$) is the rate constant of sorption, q_e (mmol g^{-1}) is the amount of metal sorbed at equilibrium, and q_t (mmol g^{-1}) is the amount of metal ion sorbed at time t (min). By plotting t/q_t versus t , v_o and q_e can be obtained from the intercept and slope, respectively as shown in **Figure 7**. They were calculated to find that their values were: $v_o = 2.272 \text{ mmol g}^{-1} \text{min}^{-1}$, $q_e = 2.380$

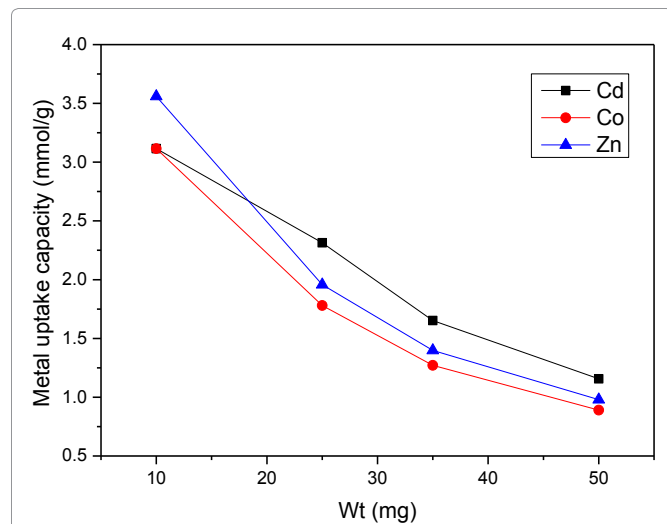


Figure 8: Effect of weight of SCMNP on metal uptake capacity of Cd(II), Co(II), and Zn(II).

mmol g⁻¹, $k = 0.40 \text{ g mmol}^{-1}\text{min}^{-1}$ for Cd(II), $v_o = 0.952 \text{ mmol g}^{-1}\text{min}^{-1}$, $q_e = 2.080 \text{ mmol g}^{-1}$, $k = 0.22 \text{ g mmol}^{-1}\text{min}^{-1}$ for Zn(II), and $v_o = 1.153 \text{ mmol g}^{-1}\text{min}^{-1}$, $q_e = 1.840 \text{ mmol g}^{-1}$, and $k = 0.34 \text{ g mmol}^{-1}\text{min}^{-1}$ for Co(II). Calculated values of q_e (2.380, 2.080, 1.840 mmol g⁻¹) match very well with the experimental values (2.314, 1.958, 1.780 mmol g⁻¹) and the correlation coefficient is above 0.99 for the three metals, respectively. All these data confirm that this model can be applied for the entire adsorption process and corroborate the sorption of the three metals on the surface of SCMNP.

Effect of weight of nano-adsorbent: The effect of SCMNP amount was also studied to illustrate the relationship between Cd(II), Zn(II), and Co(II) adsorption and mass of SCMNP, Figure 8. The weight of SCMNP was varied from 10 mg to 50 mg keeping all the other experimental variables at the optimum values. As weights of nano-adsorbent increase, the number of available adsorption sites increase until it reach saturation at 25 mg. Metal uptake capacities with 25 mg dosage of nano-adsorbent (optimum weight) for Cd(II), Zn(II), and Co(II) were 2.314, 1.952, and 1.870 mmol/g, respectively. This can be explained with the increase of surface area and the availability of the binding sites. At higher adsorbent dosage, increased number of adsorption sites enhances the uptake of metal ions. On the other hand, the adsorption capacity decreased with the increase in adsorbent mass, this behavior could be explained by the high ratio of the active sites relative to the metal ions,

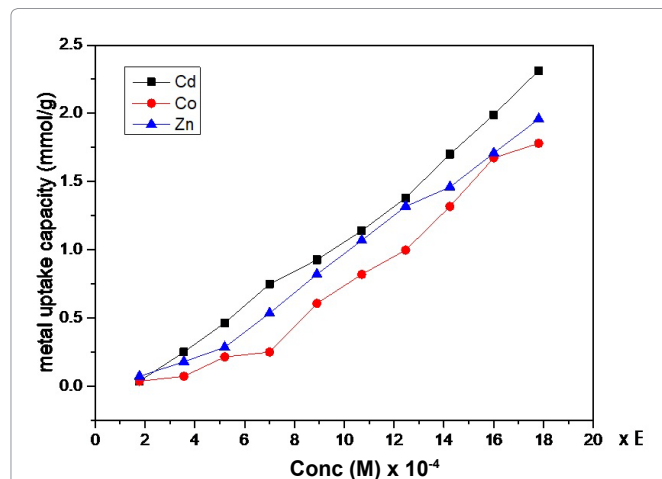


Figure 9: Effect of concentration of the solution on metal uptake capacity of Cd(II), Co(II), and Zn(II) using SCMNP.

which decreases the saturation of the active sites. In addition, the agglomeration of the nano-adsorbent particles (because of London interaction) at high dosage might also have a negative effect on the adsorption capacity [10,26].

Effect of metal ion concentration: The effect of concentration of metal ion on metal uptake was studied at concentrations from 2×10^{-4} to 2×10^{-3} M with nano-adsorbent weight of 25 mg, pH 5.0 for Cd(II) and Co(II), and 6.0 for Zn(II), and contact time of 10 min. At lower metal concentration, the ratio of number of moles of metal ion in solution to the available surface area is low and hence binding is independent of initial concentration. At higher concentration the available sites for binding is less and hence metal removal is dependent on the initial concentration. The results showed that metal uptake capacity increased with increasing of concentration of metal ion as shown in Figure 9. This indicates that metal uptake is highly dependent on the metal ion initial concentration.

The adsorption isotherms of Cd(II), Zn(II), and Co(II) could be analyzed by models given by Langmuir and Freundlich. The equation of Langmuir is applied to monolayer sorption with a completely homogeneous surface and a finite number of identical sites, is often applicable for a negligible interaction between the adsorbed molecules.

$$\frac{C_e}{q_e} = \frac{C_e}{q_m} + \frac{K_{ads}}{q_m} \quad (7)$$

Where, C_e and q_e represent the equilibrium concentrations of the adsorbate in the liquid and ad-

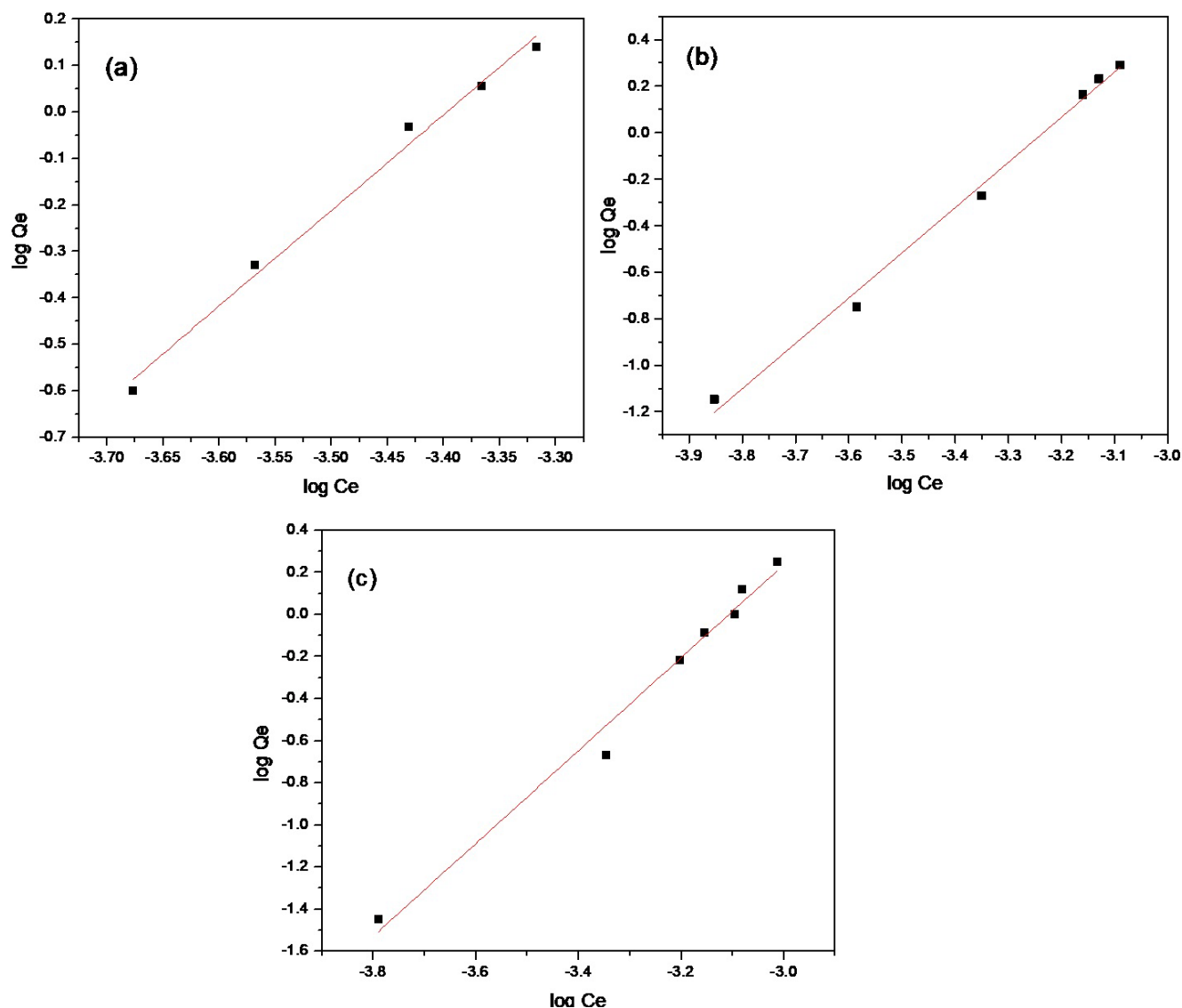


Figure 10: Freundlich plot for adsorption capacity of a) Cd(II); b) Zn(II); and c) Co(II) using SCMNPs.

sorbed phase in mmol ml^{-1} and mmol g^{-1} , respectively. q_m and k_{ads} are Langmuir constants which are related to the maximum sorption capacity (mmol g^{-1}) and the affinity of binding sites (ml mmol^{-1}), respectively, and can be calculated from the intercept (k_{ads}/q_m), and slope ($1/q_m$) of the linear plot, C_e/q_e vs. C_e .

The Freundlich equation was first used to describe gas phase adsorption and solute adsorption. In 1909, German scientist Freundlich proved an empirical relationship between the amount of gas adsorbed by a unit mass of solid adsorbent and pressure at a particular temperature. The Freundlich isotherm model assumes neither limited levels of sorption nor homogeneous site energies.

Freundlich equation in the linear form identified as follows:

$$q_e = k_f \cdot C_e^{1/n} \quad (8)$$

By taking log the equation becomes:

$$\log q_e = \log k_f + \frac{1}{n} \log C_e \quad (9)$$

Here, k_f and n are Freundlich constants, they are indicators of the sorption capacity and sorption intensity, respectively by drawing a plot of $\log q_e$ vs. $\log C_e$, the plot has slope with a value of $1/n$, and an intercept of $\log k_f$, Figure 10. Values of k_f were (9.33×10^6 , 1.90×10^6 , 7.07×10^6), values of n were (0.48, 0.51, 0.45), values of R^2 were (0.989, 0.992, 0.982) for Cd(II), Zn(II), and Co(II) respectively. It was observed from the isotherm and the correlation coefficient that the fit is better with the Freundlich model.

Stability and Reusability of the nano-adsorbent

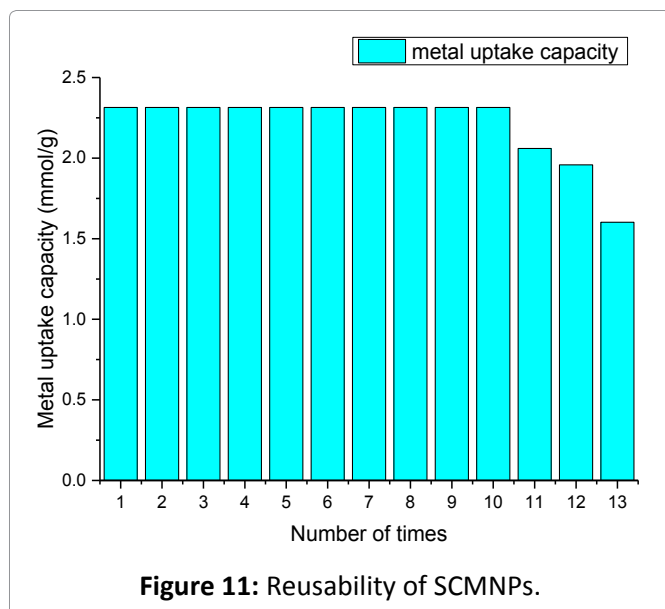


Figure 11: Reusability of SCMNP.

The study of the effect of acidic medium on SCMNP represents a significant practical application point to show the stability of this nano-adsorbent. SCMNP were found to have experienced pronounced stability under the effect of acidic medium even after a long contact time. In practical experiment, we found that the hydrolysis percentages were 0.0%, 1.5% and 4.6% when the phase was treated with concentrations of 0.1, 0.3 and 0.5M of hydrochloric acid, respectively. The percentage of the hydrolysis when it was impregnated overnight was equal to 4.6%.

For the possibility of reusing SCMNP, the batch recycling process was repeated till decreasing of metal capacity occurred. SCMNP exhibited good stability with a very slow decline in metal capacity as the number of experimental cycles increased. The value of the metal capacity has remained constant for ten times of recycling. By comparing to those in the first cycle, metal uptake capacity in the eleventh cycle decreased by only 10.97%, and the amount of decline in the twelfth and thirteenth times was by 12.70% and 15.38%, respectively, [Figure 11](#). It was proved that SCMNP has the ability of reusing with ease of regeneration for multiple cycles without any appreciable loss in its activity.

Removal of Cd(II) ion from real water samples by SCMNP using batch technique

To estimate the applicability of SCMNP, water from natural sources (groundwater, seawater, Nile River water, and drinking tap water samples) has been analyzed. From the previous batch study it was found that, Cd(II) is considered to have the

Table 1: Recovery of Cd(II) spiked real water samples with SCMNP using batch technique (Weight of SCMNP = 25.0 mg, and pH = 5.0)

Water sample	Cd(II) ion Spiked (ppm)	% Extraction
Tap water	150	97.5 ± 0.20
	100	97.2 ± 0.10
	50	96.0 ± 0.10
Ground water	150	97.0 ± 0.05
	100	96.3 ± 0.10
	50	95.0 ± 0.20
Nile River water	150	97.3 ± 0.10
	100	97.0 ± 0.20
	50	96.4 ± 0.10
Sea water	150	96.4 ± 0.05
	100	95.5 ± 0.20
	50	95.0 ± 0.20

highest metal uptake capacity value, therefore it was selected to test the feasibility of applying SCMNP to purify natural water samples after spiking with its different concentrations (50, 100, 150 ppm). The results obtained after the third run of batch technique are included in [Table 1](#). A good recovery values were achieved that ranged from 95.0% to 97.5%.

Comparison of adsorption capacity, contact time, and particle size of SCMNP with other adsorbents in removing heavy metal ions

The advantages of the synthesized SCMNP in comparison with other reported works were compiled in [Table 2](#), [Table 3](#) and [Table 4](#). It includes the high efficiency of SCMNP with respect to time required for equilibrium, and size of the adsorbent. SCMNP have produced outstanding results in removing Cd(II), Zn(II) and Co(II) ions from aqueous solutions comparing with recently used adsorbents. From these tables we can conclude that SCMNP can remove heavy metals efficiently with high values of metal uptake capacity (260.11, 128.03, 104.89 mg/g for Cd(II), Zn(II), and Co(II) respectively), very short contact time (10 min), and with very small nanosized particles (11.7-24.81 nm).

Conclusion

- SCMNP have been used to remove some toxic heavy metal ions with high metal uptake capacity values. This magnetic nano-adsorbent was prepared using microwave technique that has the economic and benign advantages of simplic-

Table 2: Comparison of the adsorption capacity, contact time, and particle size of SCMNPs with similar adsorbents in removing of Cd(II).

Adsorbent	Adsorption capacity mg/g	Contact time	Particle size of adsorbent	Ref.
Aluminosilicates	42.7-57.9	20 h	0.2-2.18 mm	[27]
Calcite	18.52	10 min	100 mesh	[28]
Chromite mine over burden	22.47	30 min	-	[29]
Iron ore slime	34.75	-	-	[30]
Low grade manganese ore	59.17	7 h	0.152 mm	[31]
Manganese nodule residue	21.2	1h	150 Mesh B.S.S passed Particles (100% < - 100 µm)	[32]
Nickel laterite (high iron)	13.2	1 h	100% < 100 µm (-150 mesh)	[33]
Nickel laterite (low iron)	11	1 h	100% < 100 µm (-150 mesh)	[33]
Nickel, leaching residue	25	-	Smaller than 20 µm	[34]
Palygorskite	4.54	1 h	200 mesh	[35]
Perlite	0.64	6 h	1.7 mm	[36]
Red bauxite	38.77	-	-	[32]
Silica, mesoporous	111.3 ± 3.3	1 h	2-50 nm	[37]
Silicate MCM-41, mesoporous	100	1 h	2-50 nm	[37]
Oxidized MWCNTs	25.7	45 min	Outer diameters = 20-30 nm Inner diameters = 5-10 nm Length between 5 and 200 µm	[38]
SCMNPs	260.11	10 min	11.7-24.81 nm	Current study

Table 3: Comparison of the adsorption capacity, contact time, and particle size of SCMNPs with similar adsorbents in removing of Zn(II).

Adsorbent	Adsorption capacity mg/g	Contact time	Particle size of adsorbent	Reference
Bentonite	52.91	15 min	0.160-0.630 mm	[39]
Activated alumina	13.69	30 min	-	[40]
Natural zeolite	2.21	40 min	1-3 mm	[41]
Bagasse fly ash modified activated carbon (10 °C)	24.06	75 min	200-250 µm	[42]
Bagasse modified activated carbon (25 °C)	31.11	12 h	< 325 mesh	[43]
Bagasse modified activated carbon (40 °C)	54	12 h	< 325 mesh	[43]
Coal fly ash unmodified (30-60 °C)	6.5-13.3	45 min	47.9 µm	[44]
Fe impregnated fly ash modified FeCl ₃ (30-60 °C)	7.5-15.5	45 min	47.9 µm	[44]
Al impregnated fly ash modified Al(NO ₃) ₃ (30-60 °C)	7.0-15.4	45 min	47.9 µm	[44]
SCMNPs	128.03	10 min	11.7-24.81 nm	(current study)

ity, rapidity and free organic solvents.

- The experimental controlling parameters affecting the metal ions uptake were studied and optimized and the results confirmed the heavily dependence on reaction pH, adsorbent dosage, contact time and metal ions concentrations.
- Adsorption isotherm study revealed that the adsorption process was fitted well with Freundlich model. In addition, it was found that the pseudo-second-order rate model described the

kinetic data more accurately.

- Stability of SCMNPs was investigated with provided excellent results. Also, regeneration studies confirmed the possibility of SCMNPs reuse without significant decrease in its efficiency.
- The SCMNPs were applied to purify different natural water samples and gave high recovery efficiencies.
- SCMNPs is considered as a promising magnetic

Table 4: Comparison of the adsorption capacity, contact time, and particle size of SCMNPs with similar adsorbents in removing of Co(II).

Adsorbent	Adsorption capacity mg/g	Contact time	Particle size of adsorbent	Reference
Al-pillared bentonite clay	38.6	24 h	-80 + 230	[45]
Kaolinite	0.919	2 h	-200 mesh	[46]
Coir pith	12.82	2 h	300-600 μm	[47]
Sulphurised activated carbon	153.6	4 h	-80 + 230 mesh	[48]
Almond green hull	45.5	7 min	< 44 μm	[49]
PFB1 (fungal based biosorbent)	190	24 h	---	[50]
Natural zeolites	14.38	5.5 h	63-106 μm	[51]
Synthetic hydroxyapatit	20.19	24 h	---	[52]
EDTA-modified silica gel	20	4 h	40-63, 63-200 μm	[53]
Lemon peel nano-adsorbent	22	10 h	BSS 150-200 mesh	[14]
Magnetic chitosan Nano-adsorbent	27.5	1 min	13.5 nm	[54]
SCMNPs	104.89	10 min	11.7-24.81 nm	(current study)

nano-adsorbent when modifying its surface with different organic compounds rich in functional groups for purposes to improve the process of removing the pollutants from aqueous medium. Really, this idea is currently being worked on in our lab.

Acknowledgment

The Chemistry Department in Faculty of Science Minia University is gratefully acknowledged for supporting this study.

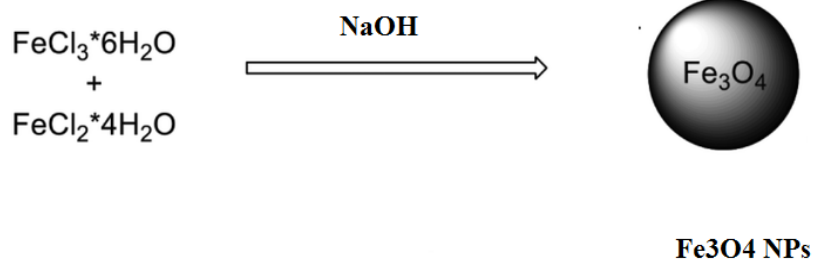
References

- Neyaz N, Siddiqui WA, Nair KK (2014) Application of surface functionalized iron oxide nanomaterials as a nanosorbents in extraction of toxic heavy metals from ground water: A review. *International Journal of Environmental Sciences* 4: 472-483.
- Shen Y, Tang J, Nie ZH, Wang D, Ren Y, et al. (2009) Preparation and application of magnetic Fe_3O_4 nanoparticles for wastewater purification. *Separation and Purification Technology* 68: 312-319.
- Jamali-Behnam F, Asghar Najafpoor A, Davoudi M, Rohani-Bastami T, Alidadi H, et al. (2018) Adsorptive removal of arsenic from aqueous solutions using magnetite nanoparticles and silica-coated magnetite nanoparticles. *Environmental Progress & Sustainable Energy* 37: 951-960.
- Iranmanesh M, Hulliger J (2017) Magnetic separation: Its application in mining, waste purification, medicine, biochemistry and chemistry. *Chem Soc Rev* 46: 5925-5934.
- Dash M (2013) Silica coated magnetite nanoparticles for removal of heavy metal ions from polluted waters.
- Moliner-Martínez Y, Ribera A, Coronado E, Campíns-Falcó P (2011) Preconcentration of emerging contaminants in environmental water samples by using silica supported Fe_3O_4 magnetic nanoparticles for improving mass detection in capillary liquid chromatography. *Journal of Chromatography A* 1218: 2276-2283.
- Tahergerabi M, Esrafilia A, Kermani A, Shirzad-Siboni M (2016) Application of thiol-functionalized mesoporous silica-coated magnetite nanoparticles for the adsorption of heavy metals. *Desalination and Water Treatment* 57: 19834-19845.
- Konate A, He X, Zhang Z, Ma Y, Zhang P, et al. (2017) Magnetic (Fe_3O_4) nanoparticles reduce heavy metals uptake and mitigate their toxicity in wheat seedling. *Sustainability* 9: 790.
- Ge F, Meng Li M, Ye H, Xiang Zhao B (2012) Effective removal of heavy metal ions Cd^{2+} , Zn^{2+} , Pb^{2+} , Cu^{2+} from aqueous solution by polymer-modified magnetic nanoparticles. *Journal of Hazardous Materials* 211-212: 366-372.
- Taha A, Shreadah MA, Ahmed AM, Heibab HF (2016) Multi-component adsorption of Pb (II), Cd (II), and Ni (II) onto Egyptian Na-activated bentonite; equilibrium, kinetics, thermodynamics, and application for seawater desalination. *Journal of Environmental Chemical Engineering* 4: 1166-1180.
- Carlos L, Einschlag F, González M, Mártire D (2013) Applications of magnetite nanoparticles for heavy metal removal from wastewater. *Waste Water-Treatment Technologies and Recent Analytical Developments* 2013: 63-77.

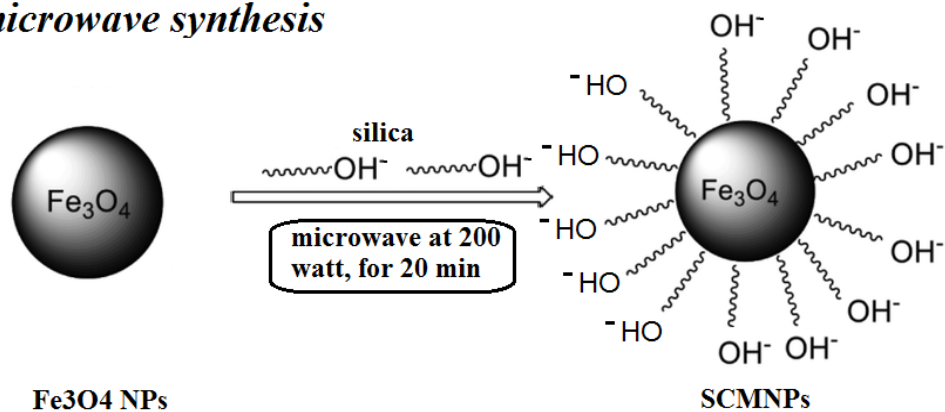
12. Zhou L, Gao C, Xu W (2010) Magnetic dendritic materials for highly efficient adsorption of dyes and drugs. *ACS Appl Mater Interfaces* 2: 1483-1491.
13. Veli S, Alyüz B (2007) Adsorption of copper and zinc from aqueous solutions by using natural clay. *J Hazard Mater* 149: 226-233.
14. Bhatnagar A, Minocha A, Sillanpää M (2010) Adsorptive removal of cobalt from aqueous solution by utilizing lemon peel as biosorbent. *Biochemical Engineering Journal* 48: 181-186.
15. Johri N, Jacquillet G, Unwin R (2010) Heavy metal poisoning: the effects of cadmium on the kidney. *Biometals* 23: 783-792.
16. Barakat M (2011) New trends in removing heavy metals from industrial wastewater. *Arabian Journal Of Chemistry* 4: 361-377.
17. Lee D-W, Fatima H, Kim K-S (2018) Preparation of silica coated magnetic nanoparticles for bioseparation. *J Nanosci Nanotechnol* 18: 1414-1418.
18. Fajaroh F, Setyawan H, Nur A, Lenggoroc WI (2013) Thermal stability of silica-coated magnetite nanoparticles prepared by an electrochemical method. *Advanced Powder Technology* 24: 507-511.
19. Ahmed SA, Soliman EM (2013) Silica coated magnetic particles using microwave synthesis for removal of dyes from natural water samples: Synthesis, characterization, equilibrium, isotherm and kinetics studies. *Applied surface science* 284: 23-32.
20. Yamaura M, Camilo RL, Sampaio LC, Macêdoc MA, Nakamura M, et al. (2004) Preparation and characterization of (3-aminopropyl)triethoxysilane-coated magnetite nanoparticles. *Journal of Magnetism and Magnetic Materials* 279: 210-217.
21. Heiba HF, Taha AA, Mostafa AR, Mohamed LA, Fahmy MA (2020) Preparation and characterization of novel mesoporous chitin blended MoO_3 -montmorillonite nanocomposite for Cu (II) and Pb (II) immobilization. *Int J Biol Macromol* 152: 554-566.
22. Almeida R, Guiton T, Pantano CG (1990) Characterization of silica gels by infrared reflection spectroscopy. *Journal of Non-Crystalline Solids* 121: 193-197.
23. Bagheri H, Afkhami A, Saber-Tehrani M, Khoshsafar H (2012) Preparation and characterization of magnetic nanocomposite of Schiff base/silica/magnetite as a preconcentration phase for the trace determination of heavy metal ions in water, food and biological samples using atomic absorption spectrometry. *Talanta* 97: 87-95.
24. Rengaraj S, Yeon K-H, Moon S-H (2001) Removal of chromium from water and wastewater by ion exchange resins. *J Hazard Mater* 87: 273-287.
25. Heiba HF, Taha AA, Mostafa AR, Mohamed LA, Fahmy MA (2018) Synthesis and characterization of CMC/MMT nanocomposite for Cu^{2+} sequestration in wastewater treatment. *Korean J Chem Eng* 35: 1844-1853.
26. Taha AA, Shreadah MA, Heiba HF, Ahmed AM (2017) Validity of Egyptian Na-montmorillonite for adsorption of Pb^{2+} , Cd^{2+} and Ni^{2+} under acidic conditions: Characterization, isotherm, kinetics, thermodynamics and application study. *Asia-Pacific Journal of Chemical Engineering* 12: 292-306.
27. Davila-Rangel J, Solache-Ríos M, Badillo-Almaraz V (2005) Comparison of three Mexican aluminosilicates for the sorption of cadmium. *Journal of Radioanalytical and Nuclear Chemistry* 267: 139-145.
28. Guzel R, Aydin F, Tegin I, Ziyadanogullari R (2007) Removal of cadmium and lead from aqueous solution by calcite. *Polish Journal of Environmental Studies* 16: 467-471.
29. Mohapatra M, Anand S (2007) Studies on sorption of Cd (II) on Tata chromite mine overburden. *Journal of Hazardous Materials* 148: 553-559.
30. Mohapatra M, Rout k, Mohapatra BK, Anand S (2009) Sorption behavior of Pb (II) and Cd (II) on iron ore slime and characterization of metal ion loaded sorbent. *Journal of Hazardous Materials* 166: 1506-1513.
31. Mohapatra M, Khatun S, Anand S (2008) Adsorption of heavy metal ions on manganese nodule-A comparative study. *Pollution Res* 25: 563-568.
32. Rout K, Mohapatra M, Mohapatra BK, Anand S (2009) Pb (II), Cd (II) and Zn (II) adsorption on low grade manganese ore. *International Journal of Engineering, Science and Technology* 1: 106-122.
33. Mohapatra M, Anand S (2007) Cd (II) adsorption on high iron containing lateritic ore of Orissa. *Indian Journal of Environmental Protection* 27: 509.
34. Václavíková M, Gallios GP (2006) Removal of cadmium, zinc, lead and copper by sorption on leaching residue from nickel production. *Acta Montanistica Slovaca* 11: 393-396.
35. Álvarez-Ayuso E, García-Sánchez A (2007) Removal of cadmium from aqueous solutions by palygorskite. *Journal of Hazardous Materials* 147: 594-600.
36. Mathialagan T, Viraraghavan T (2002) Adsorption of cadmium from aqueous solutions by perlite. *Journal of Hazardous Materials* 94: 291-303.

37. Syunichi Oshima, Jilka M Perera, Kathy A Northcott, Hisao Kokusen, Geoffrey W Stevens, et al. (2006) Adsorption behavior of cadmium (II) and lead (II) on mesoporous silicate MCM-41. *Separation Science and Technology* 41: 1635-1643.
38. Vuković GD, Marinković AD, Čolić M, Ristić MĐ, Aleksić R, et al. (2010) Removal of cadmium from aqueous solutions by oxidized and ethylenediamine-functionalized multi-walled carbon nanotubes. *Chemical Engineering Journal* 157: 238-248.
39. Mellah A, Chegrouche S (1997) The removal of zinc from aqueous solutions by natural bentonite. *Water Research* 31: 621-629.
40. Maather F Sawalha, Jose R Peralta-Videa, Jaime Romero-González, Maria Duarte-Gardea, Jorge L Gardea-Torresdey (2007) Thermodynamic and isotherm studies of the biosorption of Cu(II), Pb(II), and Zn(II) by leaves of saltbush (*Atriplex canescens*). *The Journal of Chemical Thermodynamics* 39: 488-492.
41. Motsi T, Rowson N, Simmons M (2009) Adsorption of heavy metals from acid mine drainage by natural zeolite. *International Journal of Mineral Processing* 92: 42-48.
42. Gupta VK, Ali I (2000) Utilisation of bagasse fly ash (a sugar industry waste) for the removal of copper and zinc from wastewater. *Separation and Purification Technology* 18: 131-140.
43. Mohan D, Singh KP (2002) Single- and multi-component adsorption of cadmium and zinc using activated carbon derived from bagasse-an agricultural waste. *Water Research* 36: 2304-2318.
44. Banerjee S, Jayaram R, Joshi M (2003) Removal of nickel(II) and zinc(II) from wastewater using fly ash and impregnated fly ash. *Separation Science and Technology* 38: 1015-1032.
45. Manohar D, Noeline B, Anirudhan T (2006) Adsorption performance of Al-pillared bentonite clay for the removal of cobalt(II) from aqueous phase. *Applied Clay Science* 31: 194-206.
46. Yavuz Ö, Altunkaynak Y, Güzel F (2003) Removal of copper, nickel, cobalt and manganese from aqueous solution by kaolinite. *Water Research* 37: 948-952.
47. Harshala Parab, Shreeram Joshi, Niyoti Shenoy, Arvind Lali, Sarma US, et al. (2006) Determination of kinetic and equilibrium parameters of the batch adsorption of Co(II), Cr(III) and Ni(II) onto coir pith. *Process Biochemistry* 41: 609-615.
48. Krishnan KA, Anirudhan T (2008) Kinetic and equilibrium modelling of cobalt(II) adsorption onto bagasse pith based sulphurised activated carbon. *Chemical Engineering Journal* 137: 257-264.
49. Ahmadpour A, Tahmasbic M, Bastami TR, Besharati JA (2009) Rapid removal of cobalt ion from aqueous solutions by almond green hull. *Journal of Hazardous Materials* 166: 925-930.
50. Suhasini I, Sriram G, Asolekar SR, Sureshkumar GK (1999) Biosorptive removal and recovery of cobalt from aqueous systems. *Process Biochemistry* 34: 239-247.
51. Erdem E, Karapinar N, Donat R (2004) The removal of heavy metal cations by natural zeolites. *Journal of Colloid and Interface Science* 280: 309-314.
52. Smičiklas I, Dimovic S, Plecas I, Mitric M (2006) Removal of Co²⁺ from aqueous solutions by hydroxyapatite. *Water Research* 40: 2267-2274.
53. Eveliina Repo, Tonni Agustiono Kurniawan, Jolanta K Warchol, Mika ET Sillanpää (2009) Removal of Co(II) and Ni(II) ions from contaminated water using silica gel functionalized with EDTA and/or DTPA as chelating agents. *Journal of Hazardous Materials* 171: 1071-1080.
54. Chang Y-C, Chang S-W, Chen D-H (2006) Magnetic chitosan nanoparticles: Studies on chitosan binding and adsorption of Co(II) ions. *Reactive and Functional Polymers* 66: 335-341.

(a) *co-precipitation synthesis*



(b) *microwave synthesis*



Scheme 1: Co-precipitation and microwave synthesis of SCMNPs.